Chemical Geology 451 (2017) 17–24

Contents lists available at ScienceDirect

Chemical Geology

journal homepage: www.elsevier.com/locate/chemgeo

Measurements of bacterial mat metal binding capacity in alkaline and carbonate-rich systems

Shannon L. Flynn [a,*], Qiyang Gao [a,b], Leslie J. Robbins [a], Tyler J. Warchola [a], Johanna N.J. Weston [a,c], Md. Samrat Alam [a], Yuxia Liu [a], Kurt O. Konhauser [a], Daniel S. Alessi [a]

[a] Department of Earth and Atmospheric Sciences, University of Alberta, Edmonton, AB T6G 2E3, Canada
[b] Department of Chemical Engineering and Applied Chemistry, University of Toronto, Toronto, ON M5S 3E5, Canada
[c] Deparment of Science, University of Alberta Augustana Faculty, Camrose, AB T6B 1T3, Canada

ARTICLE INFO

Article history:
Received 2 September 2016
Received in revised form 22 December 2016
Accepted 4 January 2017
Available online 6 January 2017

Keywords:
Bacterial mats
Reactivity
Metal adsorption
Alkaline
Carbonates
Geochemistry
Biogeochemistry

ABSTRACT

Measuring the metal binding potential and reactivity of bacterial mats is challenging in alkaline and carbonate-rich systems. Traditional methods used to measure these parameters, such as potentiometric titrations and metal adsorption pH edges, are difficult to implement due to the presence of the carbonate minerals that buffer pH and prevent assessment of mat surface reactivity. Additionally, under alkaline conditions metals may form hydroxide and/or carbonate precipitates. In this study we examined the metal binding capacity of four distinct bacterial mats collected from Fairmont Hot Springs, BC, Canada. To prevent metal precipitation, the bacterial mat concentration was varied under a constant initial cadmium (Cd) concentration of 8.89 μM and at pH 8. In addition to the intact bacterial mats, a carbonate mineral sample and two bacterial mats in which the carbonate mineral was removed via acid-treatment, were used as end-members to assess the mechanisms of reactivity in the whole system. Freundlich adsorption isotherms were used to fit metal adsorption data and directly compare surface reactivity among intact mats and mat components. Two of the intact mats exhibited a higher affinity for Cd compared to the mineral at metal equilibrium concentrations above 2.5 μM, while the other two intact mats had lower affinities under all experimental conditions. Generally, we found the acid-treated mats had higher Cd adsorption capacities than the carbonate mineral. When compared to their equivalent intact mats, only one acid-treated mat had a higher affinity for Cd. Further, we modeled whether metal adsorption in the intact mats, containing microbes and carbonate mineral, could be explained by a linear combination of the observed metal uptake by the organic and inorganic components through end-member experiments. Metal adsorption additivity results were mixed. Metal uptake by one intact mat was found to be additive, while for the other mat the additive model significantly underestimated the observed Cd accumulation. Our study demonstrates the potential, as well as the limitations, of using modified metal adsorption edges to determine the metal binding affinity and surface reactivity of bacterial mats in alkaline and carbonate-rich systems.

1. Introduction

Bacteria are found in nearly every environment on Earth, and because of their ubiquity, they play an integral part in the cycling of most elements (see Konhauser, 2007 for details). The initial step in many biogeochemical processes is the adsorption of metal cations to the negatively-charged cellular surfaces (Beveridge and Murray, 1976). The adsorbed cations subsequently facilitate numerous chemical processes including metal reduction (e.g., Newman et al., 1997), oxidation (e.g., Nealson et al., 1988), interacellular accumulation (Southam and Beveridge, 1994), and in many cases, biomineralization (e.g., Ferris et al., 1986).

Significant work has been undertaken to determine the mechanisms by which metal cations bind to bacteria (Mullen et al., 1989; Fein et al., 1997; Lalonde et al., 2007; Alessi and Fein, 2010). Bacterial cell envelopes contain multiple surface functional groups that have distinct proton and metal binding capacities (Beveridge and Murray, 1980; Fein et al., 1997). Typically, potentiometric titrations of bacterial cells combined with data from bulk metal adsorption experiments to the same bacteria have been used to develop protonation models and metal surface complexation models (SCM), respectively (Cox et al., 1999; Fowle and Fein, 1999; Ngwenya et al., 2003). For the SCM approach, the proton reactivity of a suspension of bacteria is tested by potentiometric titration; that is, by adding precisely-measured aliquots of acid or base to the suspension, and measuring the pH change due to the addition of that aliquot after equilibrium has been achieved, across a wide pH range. The buffering capacity measured may then be ascribed to a

* Corresponding author.
E-mail address: flynn1@ualberta.ca (S.L. Flynn).

http://dx.doi.org/10.1016/j.chemgeo.2017.01.002
0009-2541/

number of surface functional groups with discrete binding constants (pKa) and site concentrations. Once the surface functional group concentrations and pKa value(s) have been determined, bulk metal sorption experimental data from either metal adsorption pH edges (fixed metal concentration with pH varied) or metal adsorption isotherms (fixed pH with metal concentration varied) are fitted to determine the metal binding (equilibrium) constants onto the proton-active functional groups calculated from the potentiometric titration data (Fein et al., 1997; Cox et al., 1999; Haas et al., 2001; Ngwenya et al., 2003).

While this body of work demonstrates the potential of bacteria to bind and sequester metal cations, most of these studies have focused on pure cultures of bacteria grown as suspensions under carefully controlled laboratory conditions (e.g., Teitzel and Parsek, 2003). However, most bacteria found in natural environments grow in dynamic multispecies communities, referred to as either biofilms, or their thicker versions, bacterial mats (Kolter and Greenberg, 2006; Elias and Banin, 2012). Mats are also composed of dead cells and exopolymeric substances (EPS) which have been shown increase the number surface reactive sites, measured as mmol/g, compared to the intact bacterium itself (Baker et al., 2009). The secreted EPS have metal binding properties distinct from the bacterial cells and, therefore, they also impact the adsorption of metal cations from solution by bacterial mats. For example, Spath et al. (1998) measured the distribution of adsorbed cadmium (Cd^{2+}) and zinc (Zn^{2+}) on mats collected from wastewater treatment sequencing batch biofilm reactors. The EPS was found to retain 20% of the total sorbed metal cations. This indicates that there is a substantial difference between in the behavior of bacterial mats in nature, and the individual cells that make up the mats.

In addition to being composed of bacteria and EPS, mats often incorporate detrital and authigenic or allogenic minerals into their structure (e.g., Konhauser et al., 1998; Jones et al., 2004). These minerals have their own reactivity, which can alter the overall reactivity of the mats (Konhauser and Urrutia, 1999). For instance, Lalonde et al. (2007) applied a SCM approach to model the surface reactivity of intact mats from an alkaline hydrothermal spring in Yellowstone National Park. To determine the mat reactivity they performed acid titrations from pH 10 to 4, on both intact and acid treated mats. They found that the surface reactivity of the intact mats was dominated by a single surface site with a modeled pKa of approximately 7, which they attributed to the presence of incorporated carbonate precipitates. With the majority of carbonate precipitates removed, the acid treated mats exhibited an order of magnitude less buffering capacity (measured as mmol protons consumed per g mat) distributed across the tested pH range of 4 to 10. While that study was able to determine the relative buffering capacity of the mats, the authors never removed all of the carbonate minerals, meaning that even in their acid treated mat the carbonate minerals likely made a substantial contribution to the overall buffering capacity measured. Additionally, since titrations were only preformed in a single direction, the reversibility of the system was undetermined. If carbonate dissolution occurred during acid titration, a reverse titration (with base) would have shown hysteresis in the buffering capacity between the forward and reverse titration curves due to this loss of carbonate mineral. The study by Lalonde et al. (2007) highlights the difficulties in determining reactivity in alkaline and carbonate systems and our inability to use potentiometric titrations in the presence of carbonate precipitates or other pH sensitive precipitates.

In this study, we quantify the reactivity of four different bacterial mats collected from the outflow of an alkaline hot spring located at Fairmont Hot Springs, British Columbia. Because of the reasons described above, traditional methods to probe reactivity, such as potentiometric titrations, adsorption isotherms, and adsorption pH edges, are likely to be incompatible due to potential interferences caused by the rich abundance of carbonate minerals and the alkaline conditions of Fairmont Hot Springs (Rainey and Jones, 2009). Based on the results of Lalonde et al. (2007), the dissolution of carbonate minerals intertwined with the bacterial component of the intact mats during acid titrations would likely dominate the proton buffering capacity and thereby obscure direct measurement of the proton reactivity of the bacteria in the mat (Warchola et al., in review), which is ultimately key in quantifying the contribution of mat bacteria to overall observed metal removal from solution. Additionally, during metal adsorption pH edge experiments, the presence of buffering carbonates would limit the pH range able to be tested. Methods such as metal sorption edges, which are conducted under alkaline conditions, often create conditions in which formation and precipitation of carbonate and hydroxide minerals are favorable. For example, in a system in equilibrium with otavite ($CdCO_3$), the total Cd in solution decreases exponentially as a function of increased pH (Fig. 1). In this case Cd and otavite are used as proxies for divalent metals and their carbonate precipitates, and clearly illustrate that under increasingly alkaline conditions greater divalent cation precipitation can be expected. Accordingly, this precludes the investigation of metal adsorption using traditional metal adsorption isotherms for alkaline conditions.

As metal adsorption and the reactivity of bacterial mats are understudied in carbonate rich and alkaline systems, in this study, we propose a method to bypass the issues posed by traditional methods. To address these issues, modified metal adsorption experiments (in which Cd was used as a proxy for environmentally relevant divalent metals) were used to quantify the reactivity of the bacterial mats from a carbonate-rich system under metabolically inactive conditions. To minimize Cd precipitation, the concentration of sorbent (the bacterial mat or mineral) was varied with a constant initial Cd concentration in lieu of varying the metal concentration. Adsorption is thought to be a fast process occurring on a time scale of seconds to minutes (Xue et al., 1988; Kuyucak and Volesky, 1989; Matheickal et al., 1999), whereas precipitation of mineral phases is the slower step on a time scale of hours to days (Sadiq, 1992). Therefore, the length of Cd exposure was limited to 4 h to allow for adsorption to reach equilibrium and to exclude significant precipitation of Cd as carbonates or hydroxides. In addition to determining the reactivity of intact bacterial mats, reactivity was also determined for travertine (a lithified carbonate sediment associated with microbial mats in hot springs) and two of the bacterial mats that were acid treated to remove the incorporated carbonate minerals. The reactivity of the intact bacterial mats, endmember mineral component, and pure bacterial components (acid treated mats) was quantified through the Cd sequestration potential. By quantifying the potential of not just the intact mats but each endmember component, the contribution of each endmember to the overall observed Cd sequestration in intact mat samples was assessed.

2. Methods

2.1. Handling and collection of samples

Bacterial mats and travertine samples were collected from an alkaline hot spring located at Fairmont Hot Springs, BC, Canada on

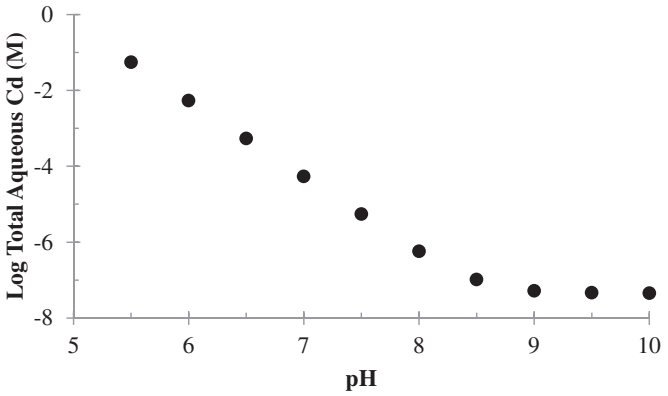

Fig. 1. Total Cd in solution in equilibrium with otavite as a function of pH.

September 2, 2015. Material was collected from four distinct bacterial mats, subsequently referred to as: black mat, green mat, spongy green mat, and orange mat (Fig. SI.1). The mats were removed from the underlying travertine and placed in polypropylene tubes submerged in water from the hot spring. In addition to bacterial mat and travertine (mineral) samples, water samples were collected for metals analysis. The pH and temperature were measured during sample collection using a Fisher Science Accumet AP71 portable dual pH and temperature meter along the hot spring flow path (locations shown in Fig. SI.1). Water samples were filtered through 0.22 μm nylon membranes and acidified with three drops of 12.1 M HCl for preservation. All samples were placed on ice before transport to the University of Alberta. Samples were stored at 2 °C prior to analyses.

2.2. Preparation of travertine sample

A travertine mineral sample, which was overlain by the bacterial mats in the field, was collected for reactivity/adsorption experiments because it represents the mineral endmember associated with the bacterial mats. Following collection, the travertine was dried in an oven at 60 °C for 24 h, then crushed and ground into a fine powder using a mortar and pestle. The powdered travertine was treated to remove any trace organics that may have been incorporated in the travertine using a modified version of the separation method described in Schofield et al. (2008). In summary, the powdered travertine was soaked in 1 M NaOH for 24 h before being repeatedly washed with 18.2 MΩ ultrapure water and centrifuged at 7000*g*; this process was repeated five times. Following washing, the travertine-water slurry was placed in a separatory funnel with hexane, shaken vigorously and left to separate overnight. The following morning the travertine powder and water was separated from the organics and hexanes, as the latter floated on top as a separate layer. The organics-free travertine was washed with 18.2 MΩ ultrapure water once more before being centrifuged and decanted twice at 7000*g* for 5 min, and a final time for 30 min to form a wet pellet. These wet pellets were subsequently used for metal adsorption experiments and a portion of the organics-free travertine was dried. The dried travertine, with a wet to dry ratio of 1.45 (SI Table 1), was analyzed for mineral composition and surface area using X-ray powder diffraction (XRD) and Brunauer-Emmett-Teller surface area analyzer (BET), respectively.

2.3. XRD

XRD analysis of the powdered mineral sample was performed using a Rigaku Geigerflex Powder X-ray diffractometer equipped with a cobalt tube, and graphite monochromator and scintillation detector. Data were analyzed using the JADE 9.1 software, with peak locations being referenced using the International Centre for Diffraction Data (ICDD) and Inorganic Crystal Structure Databases (ICSD).

2.4. Preparation of bacterial mat

All four bacterial mat samples were washed and centrifuged 3 times for 5 min at 7000*g* using a prepared stock a solution of 10 mM 4-(2-hydroxyethyl)-1-piperazineethanesulfonic acid (HEPES) buffer and 10 mM NaCl adjusted to pH 8. The bacteria were then suspended in approximately 100 mL of the previously described solution on a magnetic stir plate and pH adjusted using small aliquots of 1 M NaOH until the solution pH stabilized at 8 (the approximate ambient pH of the hot spring). Bacterial mats were then pelleted by centrifuging and decanting two times for 5 min and two times for 30 min at 7000*g* to produce a compressed wet pellet from each mat. A subsection of each mat was subsequently acid treated with a solution of 0.1 M nitric acid and 10 mM NaCl to remove carbonate minerals that may have been associated with the bacterial mats. Acid treated bacterial cells have been found to remain intact and viable without any visible difference from their untreated counterparts in previous studies (Fein et al., 1997; Borrok et al., 2004). The acid treatment was performed on a stir plate with continual additions of the 0.1 M nitric acid plus 10 mM NaCl solution, until the pH of the bacterial mat suspension had stabilized at or below pH 4.5. The acid treated mats were then pelleted using the method described above (Section 2.2). Two of the acid treated mats (green and orange) were further treated with the previously described HEPES stock solution until the pH of the bacterial mat suspension stabilized at 8. The acid treated mats were then pelleted using the method described above, and are referred to here as 'acid treated green mat' and 'acid treated orange mat'. The mass difference between the pre- and post-acid treated bacterial mat was used to determine the relative bacterial and mineral content of the intact bacterial mats.

2.5. Cd adsorption experiments

Batch Cd adsorption experiments were conducted at room temperature (20 °C) and pressure in a matrix of 10 mM HEPES and 10 mM NaCl, adjusted to pH 8. As no nutrients or electron donors were added to the experimental solutions, and the contact time in metal adsorption experiments was short (4 h), the role of potential bacterial metabolism was assumed to be minimal. In contrast to traditional adsorption experiments where the concentration of metal is varied, the concentration of Cd added was held constant at 8.89 μM (1 ppm) while the sorbent concentration was varied from 0 to 8 g/L for the travertine and 0 to 25 g/L for the bacterial mats, based on wet weight from the pelleted material. Duplicate experiments were conducted on the travertine, four intact bacterial mats, and two acid treated bacterial mats. In preparation for the experiments, bacterial mat or travertine samples were first added to the solution in polypropylene test tubes; the pH was then checked and adjusted if needed before the solution was spiked with Cd. Test tubes were rotated end-over-end at 100 rpm for 4 h, adequate time for Cd adsorption and equilibrium to be achieved but short enough to prevent significant precipitation (<1.5%, see control experiment in Fig. SI.3). The pH of the solution was measured and adjusted as needed over the first hours of the experiment. At the end of the adsorption experiment, the pH of each sample was measured and recorded, the tubes centrifuged at 5000*g* for 5 min, the resulting supernatant subsequently filtered through a 0.2 μm nylon membrane, and then diluted 1:10 with 2% nitric acid before Cd analysis.

2.6. ICP-MS analysis

Metal analyses of hot spring water and Cd from adsorption experiments were conducted at the Environmental Geochemistry Laboratory at the University of Alberta using an Agilent 8800 ICP-MS/MS. A detailed table of the analysis conditions and dilution factors used is provided in Table SI.2.

3. Results

3.1. Hot spring water, travertine and bacteria mat mineral analysis

Water samples along the flow path were found to show no systematic variation in measured chemical composition, while the pH increased 1.04 units along the sampled transect and the temperature decreased by 1.9 °C (Table SI.3). In total 14 cationic and 1 anionic elements were found to be in quantifiable concentration in hot spring water by ICP-MS/MS analysis. The primary cations in the hot spring water were Ca and Mg, with Na, K, Si, and Sr also being present in the ppm range; similar to concentrations reported by Warchola et al. (in review) for the same transect. The remaining 8 elemental concentrations were found to be in the ppb range (Table SI.3). Anions were not measured but were assumed to be similar to previous measurements from the same site by Warchola et al. (in review), in which the anions were dominated by alkalinity in the form of carbonate (380–

400 ppm), sulphate (230 ppm), and chloride (26 ppm) with a range of ionic strengths between 12 and 14 mM.

The XRD analysis of powdered travertine mineral from the hot springs was found to be composed of calcite, quartz, dolomite and rutile (Fig. SI.2). The calcite likely precipitated in response to the supersaturated state of the solution with respect to pCO_2 in water emerging from the subsurface. The dolomite is likely the product of alteration and Mg exchange in a portion of the calcite. The presence of quartz is likely the result of detrital sand grains entrapped in the carbonate travertine. Rutile, a common paint additive, could be from the inclusion of paint chips washed from the thermal pools at the resort above the sampling site.

The carbonate mineral content of each bacterial mat was determined through acid treatment (Table 1). The orange mat had the lowest carbonate mineral content, with 32.2% carbonate minerals by mass. The black and spongy green mats were found to have similar carbonate mineral contents to the orange mat with 36.5% and 39.8%, respectively. The green mat was composed of significantly more carbonate minerals with 72.8% of the mat being composed of carbonates, nearly double the content of the other bacterial mats.

3.2. Cd adsorption experiments

3.2.1. Travertine

The amount of Cd adsorbed from solution increased with increasing concentration of travertine particles until complete removal of Cd was achieved at approximately 7.7 g/L (Fig. 2). From a concentration of 0.06 g/L of travertine to 2.0 g/L, a rapid and near linear increase in the adsorption of Cd was observed. The extent of Cd adsorbed per g of travertine decreased from 2.0 g/L until 7.7 g/L of travertine where < 1% of Cd was measured to be remaining in solution. Above 7.7 g/L of travertine, near-complete removal of solution Cd was observed.

3.2.2. Bacterial mats

3.2.2.1. Green mat. Cd adsorption increased with increasing concentration of green mat until the percent adsorbed plateaued above 15.8 g/L of bacterial mat (Fig. 3A). At this concentration or greater, the percent Cd adsorbed was found to be 90–95% of the total Cd regardless of increasing concentration of bacterial mat, potentially due to the presence of organic acids in solution that complex Cd. Initially the extent of Cd adsorption, from 0.041 to 1.2 g/L of bacterial mat, was rapid and linear in increase relative to the increase in bacterial mat added. Once the green mat concentration was > 1.2 g/L, and until 15.8 g/L, the extent decreased before the percent adsorbed plateaued.

3.2.2.2. Black mat. A linear and rapid increase in adsorbed Cd was observed with increasing black mat concentrations from 0.069 to 1.13 g/L (Fig. 3B). Above 1.13 g/L of bacterial mat the extent of Cd adsorption per g/L decreased with increasing bacterial mat until 15.9 g/L of black mat. Above 15.9 g/L of bacterial mat, the percent of Cd adsorbed plateaus at 82–92% despite increasing bacterial mat concentration.

3.2.2.3. Spongy green mat. The spongy green mat showed a sharp and linear increase in Cd adsorbed with increasing bacterial mat concentration from 0.062 to 1.06 g/L (Fig. 3C). The extent of adsorption decreased with increasing spongy green mat concentration from 1.06 to 5.11 g/L bacterial mat before the percent adsorbed plateaus at 81–92% even with increasing bacterial mat concentrations.

3.2.2.4. Orange mat. Cd adsorption to the orange mat increased with increasing mat concentrations until plateauing above 11.00 g/L (Fig. 3D). The maximum adsorbed Cd was found to be between 95 and 98% of the initial concentration. At lower concentrations of the orange mat, from 0.048 to 1.12 g/L, the extent of adsorption is rapid and linear. From 1.12 to 11.00 g/L the extent of Cd adsorption decreases with increasing mat concentrations.

3.2.3. Acid treated bacterial mats

3.2.3.1. Acid treated green mat. A linear increase in Cd adsorption was observed with increasing acid treated green mat from 0.069 to 0.48 g/L (Fig. 4A). Above 0.48 to 0.99 g/L of bacterial mat, the extent of Cd adsorption decreased with increasing bacterial mat concentration. After 0.99 g/L, the percent of Cd adsorbed plateaus at 97 to 100% even with continuing additions of bacterial mat.

3.2.3.2. Acid treated orange mat. The acid treated orange mat showed a rapid and linear increase in the percent of Cd adsorbed with increasing mat concentrations from 0.034 to 0.98 g/L (Fig. 4B). The extent of increased adsorption per g/L of bacterial mat decreased from 0.98 to 8.10 g/L of bacterial mat. Once the concentration of bacterial mat reached 8.10 g/L the adsorption of Cd ranged between 91 and 100% of the initial Cd concentration.

Table 1
Partitioning of mass between bacteria and carbonate mineral in the intact bacterial mats.

	% Mineral	% Bacteria
Spongy green mat	39.8	60.2
Black mat	36.5	63.5
Orange mat	32.1	67.9
Green mat	72.8	27.2

4. Discussion

For this study, metal adsorption to travertine, bacterial mats, and acid treated bacterial mats was modeled using; (1) Freundlich isotherms as a means of determining the relative metal binding affinity, and (2) linear combination fits of the endmember component contributions to the intact mat Cd adsorption capacity as a means of testing the additivity of metal adsorption in the intact bacterial mats. Freundlich isotherms have been successfully employed to quantify the adsorption capacity of numerous biosorbents, such as marine algae (Kuyucak and Volesky, 1989), fungi (Mullen et al., 1992), and bacteria (Mullen et al., 1989; Volesky and Holan, 1995). The combined experimental data for the duplicate experiments for each sorbent was fitted together using the linearized Freundlich isotherm equation:

$$\mathrm{Log}(C^*) = \mathrm{Log}\,(K) + N * \mathrm{Log}(C) \quad (1)$$

in which C and C* represent the equilibrium Cd concentration in solution (μm) and the adsorbed Cd concentration (μm/g), respectively, and N and K are Freundlich constants. In this form, the K constant represents the affinity of the sorbent for Cd in μm/g at an equilibrium solution concentration of 1 μm. The linearized Freundlich equation fits the Cd adsorption data for environmental samples well (Table 2), with coefficient of determination values ranging from 0.86 to 0.96 (insets in Figs. 2, 3A–D, and 4A–B).

At low metal concentrations, those below 1 μM equilibrium Cd in solution, travertine shows the highest modeled affinity for Cd (see Fig. 5). The second highest affinity in this range was predicted to be for the acid treated green mat, which along with travertine at 1 μM, had an affinity that was double that of all other sorbents. Above 1 μM the affinity of travertine for Cd increases more slowly relative to the other sorbents, as indicated by the corresponding N values (Table 2). Once the equilibrium Cd solution concentration reaches 7.5 μM, the affinity of travertine for Cd is only greater than that of the intact black mat, and at or above 10 μM equilibrium Cd in solution travertine has the lowest overall Cd affinity.

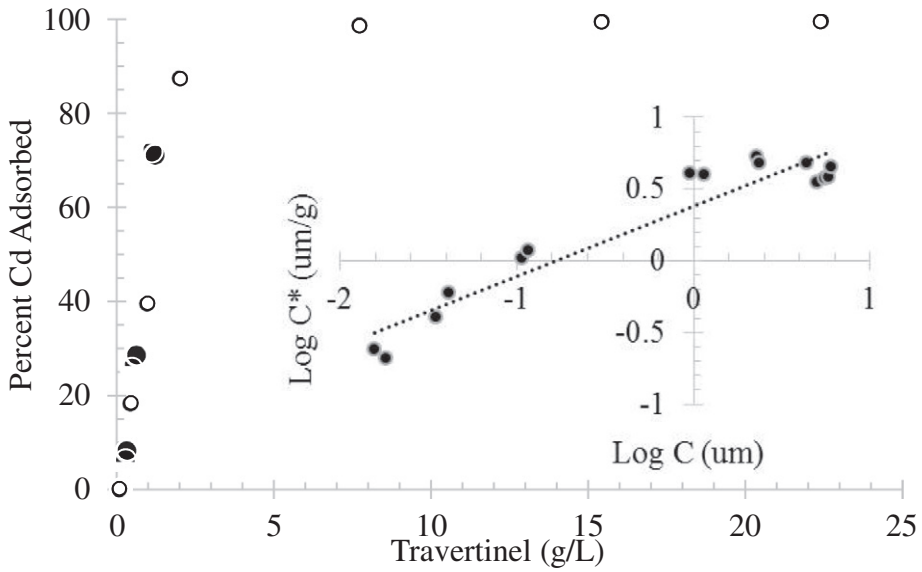

Fig. 2. Results of duplicate experiments measuring Cd adsorption onto the travertine from Fairmont Hot Springs plotted as the percentage of Cd adsorbed to the travertine as a function of Travertine concentration with the fit of the linear form of the Freundlich isotherm equation inset.

Among the intact mats, which include both the microbial biomass and carbonate solids, the orange mat has the highest Cd affinity at equilibrium concentration below 3 μM; above 3 μM the green mat has the highest affinity with the orange mat having the second highest. The spongy green and black mats are predicted by the models to have lower affinity for Cd than the green and orange mats throughout the entire examined Cd concentration range. Of these two intact mats, the black mat is predicted to have the higher affinity for Cd when the metal concentration is below 4.5 μM, and vice versa above 4.5 μM.

Of the two acid treated mats tested, the green mat has a higher predicted affinity for Cd over the entire range examined. When compared to the intact green mat, the acid treated green mat was found to have approximately twice the affinity for Cd. In contrast the acid treated orange mat exhibited lower Cd affinity, approximately half that of the intact orange mat.

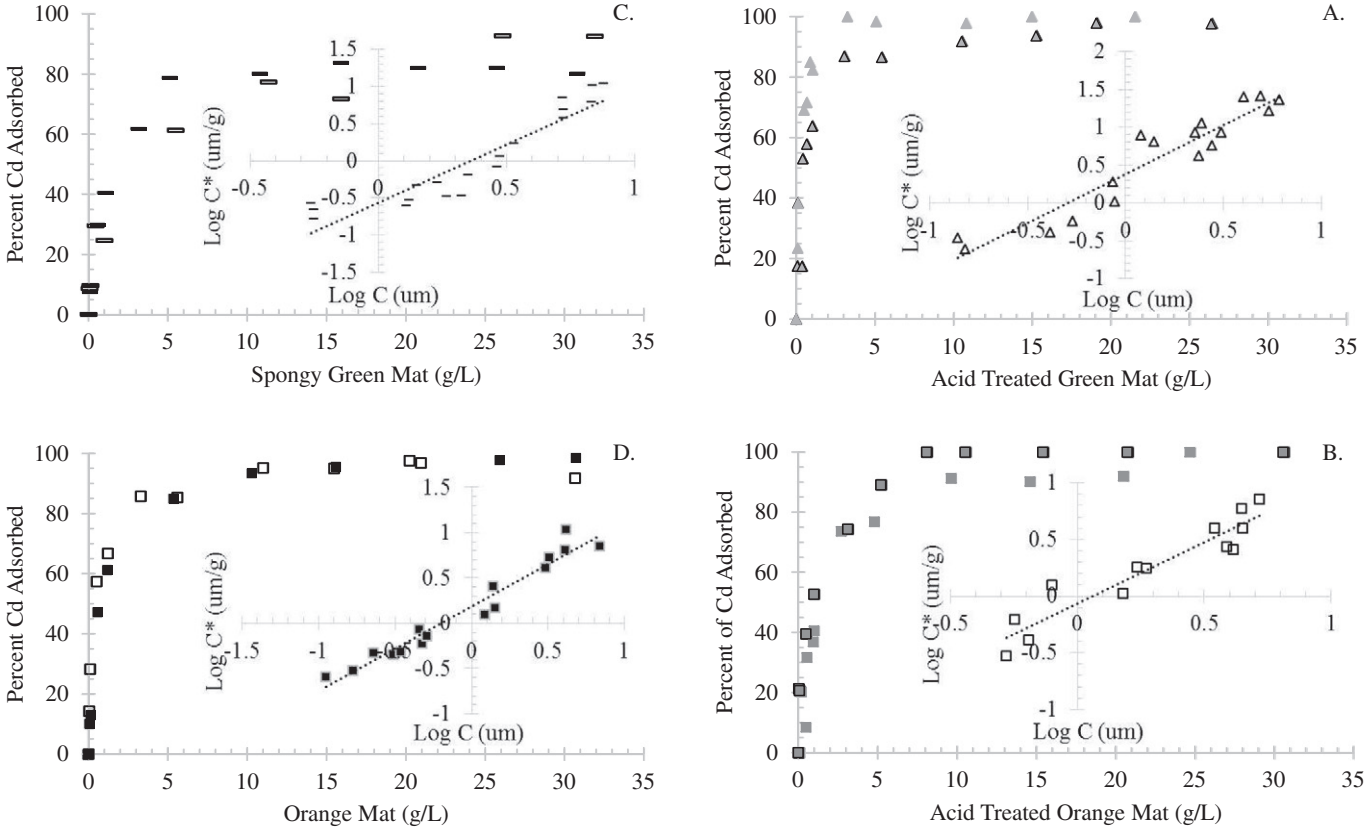

Fig. 3. Cd adsorption to each of the bacterial mats plotted as percent Cd adsorbed as a function of the bacterial mat concentration with the respective fits of their linear form of the Freundlich isotherm equation inset (A. green mat, B. black mat, C. spongy green mat, and D. orange mat).

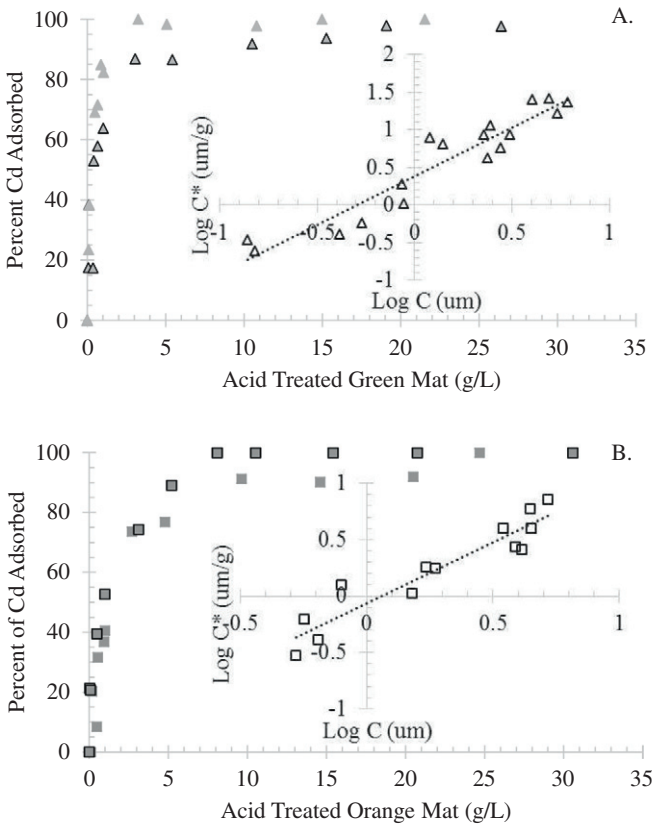

Fig. 4. Cd adsorption to the acid treated bacterial mats plotted as percent Cd adsorbed as a function of the bacterial mat concentration with the respective fits of their linear form of the Freundlich isotherm equation inset (A. acid treated green mat, B. acid treated orange mat).

To determine whether metal adsorption by the intact mats is additive (that is, if it can be modeled as the sum of its constituent components), a component additivity modeling approach utilizing acid treated mat (biomass only) and travertine-only endmembers was applied to measured Cd adsorption data from the corresponding intact mats. Using this approach, it can be determined whether Cd adsorption to the components of the intact mats is additive, or if when combined, the sum of the Cd adsorption to the individual components show synergistic or antagonistic relationships that impact overall Cd removal from solution (Alessi and Fein, 2010). A composite model composed of the sum of the adsorption capacity of individual mat components, similar to that used by Small et al. (1999) for bacteria-Fe(III) composites, was used to determine the additivity of the bacterial mats. The composite

Table 2
Freundlich isotherm fitting parameters for each sorbent with the coefficient of determination for the linear regressions for the linear fit of the experimental data, and Freundlich fitting parameters for composite and subtractive models.

	N	K	R^2
Travertine	0.45	2.41	0.91
Green mat	1.25	1.10	0.95
Orange mat	0.94	1.52	0.95
Spongy green mat	1.57	0.27	0.86
Black mat	1.19	0.48	0.96
Acid treated green	1.29	2.42	0.90
Acid treated orange	1.08	0.87	0.89
Composite green mat	0.77	2.60	
Composite orange mat	0.75	1.51	
Subtractive green mat	1.64	1.63	
Subtractive orange mat	1.26	1.03	
Subtractive spongy green mat	3.63	0.005	
Subtractive black mat	2.51	0.027	

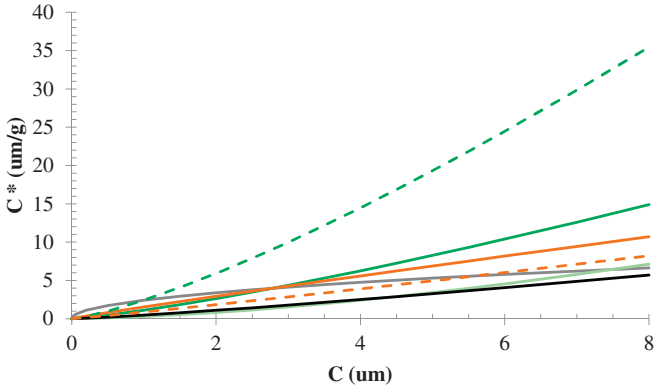

Fig. 5. Models of the predicted adsorbed Cd concentrations (C*) based on the Freundlich isotherm, including travertine mineral (grey line), green mat (dark green line), black mat (black line), Spongy green mat (light green line), orange mat (orange line), acid treated green mat (dashed green line), and acid treated orange mat (dashed orange line).

Cd removal from solution ($C^*_{Comp.}$), which represents the predicted Cd removal by intact mats, was calculated as the sum of the intact mat components, according to:

$$\%Bac. * C^*_{Bac.} + \%Min. * C^*_{Min.} = C^*_{Comp.} \quad (2)$$

in which the sum of the predicted component Cd affinity, $C^*_{Bac.}$ (acid treated bacterial mat) and $C^*_{Min.}$ (travertine) are multiplied by their respective mass percent in the intact bacterial mat. The calculated Cd removal ($C^*_{Comp.}$) was then substituted for C^* in Eq. (1) to calculate the hypothetical composite model Cd removal across a range of Cd concentrations. Overall, the composite model for the green mat reasonably matches the Freundlich fit to the intact green mat Cd adsorption data (Table 2 and Fig. SI.4A, B), but overestimates affinity for Cd at low concentrations (below 6 μm) and underestimates mat Cd affinity at higher equilibrium Cd concentrations in solution above 6.5 μm. The composite orange mat underestimates the adsorbed Cd concentration once the equilibrium solution Cd concentration is above 0.95 μM, or across the majority of the experimental range.

As a second test of the component additivity of the system, a subtractive model (Eq. (3)), was created to assess if the adsorption behavior of travertine and an intact mat could be used to calculate the adsorption behavior of the bacteria-only component of that mat, as represented by the acid treated mat. In this model, the total concentration of Cd adsorbed to the intact mat ($C^*_{Tot.}$) is subtracted by the product of the percent travertine by mass (%Min.) in the mat and the concentration adsorbed to the travertine ($C^*_{Min.}$), and then divided by the percent mass of bacteria in the intact mat determined through acid treatment (%Bac.), giving the concentration of Cd that should be adsorbed on the bacterial component of the mat ($C^*_{Bac.}$), according to:

$$\frac{C^*_{Tot.} - \%Min. * C^*_{Min.}}{\%Bac.} = C^*_{Bac.} \quad (3)$$

The subtractive models fitting parameters are shown in Eq. (2) and Fig. SI.5. The subtractive model for the green mat overestimates the affinity of the acid treated green mat for Cd, once the equilibrium solution Cd concentration is above 3.0 μM. In contrast, the subtractive model for the orange mat overestimates Cd adsorption onto the bacterial component of acid treated orange mat over the entire experimental range. The overestimation for both the subtractive green and orange mats could be caused by a difference in the size of reactive mineral particles used as the inorganic endmember and particle size found in the mats. If the particles found in the mats were smaller than those used as the mineral endmember, then the mineral contribution would have likely been

underestimated due to the difference in the reactive surface area. Another possibility is that Ca and Mg are released during travertine dissolution in the intact mats. Then, the Ca and Mg compete with Cd for adsorption to surface sites within the bacterial components of the mat. The competition is expected to be minimal as binding constants for Ca^{2+} and Mg^{2+} to the model bacterium *Bacillus subtilis* are two orders of magnitude lower than that for the binding of Cd^{2+} (Flynn et al., 2014). This underestimation would then result in the overestimation of the bacterial component contribution, as our models are too simplistic to represent the true complexity of the mat. The subtractive models for the spongy green and black mats were found to have higher N values than those for the green and orange mats, however, the K values were significantly lower. Over the range examined, the bacterial component of the green mat is modeled to have the highest Cd metal sorption followed by the bacterial component in the orange, spongy green, and black mats.

In alkaline and carbonate systems, metals can be incorporated into carbonate precipitates by either abiotic or biotic processes. Abiotic partitioning of alkali earth elements into carbonates has been found to be more significant into aragonite than calcite, with incorporation increasing with decreased ionic radius (Okumura and Yasushi, 1986). Additionally, the partitioning of divalent metals into carbonate minerals is affected by their depth in the water column (Elderfield et al., 1996) and divalent metals have been shown to coordinate at Ca sites on calcite, forming mononuclear inner-sphere adsorption complexes (Elzinga and Reeder, 2002). At present it is not known whether the same mechanism of trace metal incorporation into carbonates minerals occurs via biotic processes. However, the first step is likely adsorption of Ca^{2+} ions to the negatively charged bacterial surface sites or negatively charged bacterial mat surface sites (a combination of bacterial surface sites and EPS surface sites) (Thompson and Ferris, 1990; Braissant et al., 2007). The surface sites act as nucleation points from which carbonate minerals can grow using the bacterial surface as a template. Indeed, a number of different carbonate phases can form by simply replacing Ca for other divalent cations in the growth media, e.g., Fe^{2+} to form siderite (Mortimer et al., 1997) and Sr^{2+} to form strontianite (Schultze-Lam and Beveridge, 1994). In addition to the Ca being incorporated into the biogenic carbonate precipitates, other metals (i.e., Cd, Cu, Zn, Pb, REEs, Sr) bound to the bacterial mats could also be incorporated into the carbonate precipitates nucleating on the bacterial mat. For instance, previous studies have documented that cyanobacteria can partition of up to 1.0 wt% strontium in calcite (Ferris et al., 1995). This has important implications for trace metal incorporation into biogenic minerals in the environment because passive carbonate biomineralization may provide a useful strategy for contamination issues in Ca carbonate-rich aquifers (Warren et al., 2001).

This study demonstrates the possibility to probe and measure metal reactivity in alkaline- and carbonate-rich systems by altering traditional metal adsorption experiments – using a low and consistent initial metal concentration, varying the bacterial mat concentration, and shortening the exposure time. While this method may be expanded upon or altered to elucidate additional information about the bacterial mat reactivity, our modified metal adsorption experiments have shown the ability to determine the relative Cd affinity of several bacterial mats from a hot spring under varied metal loading conditions, and provides a first step in determining which of the metal immobilization mechanisms discussed above may be important in alkaline and carbonate-rich systems. Differences in the metal binding between the mats likely was due to the differences in the ratio of biological material to travertine/mineral phases and the ratio of bacterial cells to EPS present in the mats. The reactivity of the bacteria within the mats is not thought to be strongly influenced by the species of bacteria present, as previous work by Borrok et al. (2005) found remarkable similarities in the reactivity of 36 separate bacterial species and consortia. Our method showed mixed results in determining the relative additivity of mat biological and inorganic components toward the total reactivity of the intact mat. The mixed results with regards to system additivity may have stemmed from a variety of differences in the mats, including density of the biological material, diffusion of Cd through the mat, and detrital inorganic grain size. Further work will be needed to determine whether adsorption of metals to bacterial surface functional groups is the precursory step for metal incorporation into biogenic carbonates. Future studies are also needed to explore how the adsorption of metal onto bacterial mats affects metal incorporation to microbially-induced carbonates, and to assess the relative contribution of biotic or abiotic mechanisms to the formation of microbial mat carbonates. By continuing to study bacterial mat reactivity in alkaline- and carbonate-rich systems, we may be able to determine these controls on metal partitioning into biogenic carbonates, and thereby further our understanding of metal cycling and sequestration in relevant modern environments, ranging from hot springs to oceans.

5. Conclusions

This study demonstrates the potential and limitations of using modified metal adsorption edges to determine the metal binding affinity and surface reactivity of metabolically inactive bacteria in alkaline and carbonate-rich systems, such as in bacterial mats that have authigenic carbonate minerals. The empirical models were effective in determining which of the Fairmont Hot Springs' bacterial mats had the highest metal adsorption potential. However, the results were mixed when the additivity of the bacterial mat components, mineral, and bacteria, were measured separately and the sum of their relative contributions used to create additive models. This study highlights the potential as well as limitations of using modified metal adsorption edges to determine the metal binding affinity and surface reactivity of natural bacteria in alkaline and carbonate-rich systems.

Models such as the ones presented in this paper expand our understanding of bacterial mat reactivity in alkaline and carbonate rich systems. Further studies are required to transition from modeling reactivity in these complex systems with empirical models, such as Freundlich or Langmuir isotherms, to thermodynamic models, such as surface complexation models. The current limit in transitioning to thermodynamically driven models is our inability to measure proton reactivity in the presence of carbonate minerals and in turn to quantify the number of surface sites could adsorb metals. While metals can be used as a probe for overall mat reactivity, the reactivity of bacterial mats will vary based on the metal tested (depending on, i.e., charge and hydrodynamic radius), interactions between individual sorbents in the intact mat, and potential diffusional or kinetics effects. Therefore, further work is required to constrain proton reactivity of the biomass component of intact mats, and to provide improved methods for predicting total reactivity of mats toward metals in alkaline and carbonate rich systems.

Acknowledgements

This work was supported by Discovery Grants from the Natural Sciences and Engineering Research Council of Canada (NSERC) to Daniel Alessi (RGPIN-04134) and Kurt Konhauser (RGPIN-165831). Leslie Robbins gratefully acknowledges the support of a NSERC Vanier CGS, and Tyler Warchola a NSERC CGS-M. We also would like to acknowledge the staff of the Fairmont Hot Spring Resort for providing us with access to the site, as well as working space to set up a temporary lab. In addition, we thank the two reviewers for their insightful and pointed reviews which greatly aided in the improvement of this manuscript.

Appendix A. Supplementary data

Supplementary data to this article can be found online at http://dx.doi.org/10.1016/j.chemgeo.2017.01.002.

References

Alessi, D.S., Fein, J.B., 2010. Cadmium adsorption to mixtures of soil components: testing the component additivity approach. Chem. Geol. 270, 186–195.

Baker, M.G., Lalonde, S., Konhauser, K.O., Foght, J.M., 2009. Role of extracellular polymeric sustances in the surface chemical reactivity of Hymenobacter aerophilus, a psychrotolerant bacterium. Appl. Environ. Microbiol. 76, 102–109.

Beveridge, T.J., Murray, R.G.E., 1976. Uptake and retention of metals by cell-walls of *Bacillus subtilis*. J. Bacteriol. 127, 1502–1518.

Beveridge, T.J., Murray, R.G.E., 1980. Sites of metal-deposition in the cell wall of *Bacillus subtilis*. J. Bacteriol. 141, 876–887.

Borrok, D., Fein, J.B., Tischler, M., O'loughlin, E., Meyer, H., Liss, M., Kemner, K.M., 2004. The effects of acidic solutions and growth conditions on the adsorptive properties of bacterial surfaces. Chem. Geol. 209, 107–119.

Borrok, D., Turner, B.F., Fein, J.B., 2005. A universal surface complexation framework for modeling proton binding onto bacterial surfaces in geologic settings. Am. J. Sci. 305, 826–853.

Braissant, O., Decho, A.W., Dupraz, C., Glunk, C., Przekop, K.M., Visscher, P.T., 2007. Exopolymeric substances of sulfate-reducing bacteria: interactions with calcium at alkaline pH and implication for formation of carbonate minerals. Geology 5, 401–411.

Cox, J.S., Smith, D.S., Ferris, F.G., 1999. Characterizing heterogeneous bacterial surface functional groups using discrete affinity spectra for proton binding. Environ. Sci. Technol. 33, 4514–4521.

Elderfield, H., Bertram, C.J., Eraz, J., 1996. A biomineralization model for the incorporation of trace elements into foraminiferal calcium carbonate. Earth Planet. Sci. Lett. 142 (490-423).

Elias, S., Banin, E., 2012. Multi-specis biofilms: living with friendly neighbors. FEMS Microbiol. Rev. 36, 990–1004.

Elzinga, E.J., Reeder, R.J., 2002. X-ray absorption spectroscopy study of Cu^{2+} and Zn^{2+} adsorption complexes at the calcite surface: implications for site-specific metal incorporation preferences during calcite crystal growth. Geochim. Cosmochim. Acta 66, 3943–3954.

Fein, J.B., Daughney, C.J., Yee, N., Davis, T.A., 1997. A chemical equilibrium model for metal adsorption onto bacterial surfaces. Geochim. Cosmochim. Acta 16 (3319-3228).

Ferris, F.G., Beveridge, T.J., Fyfe, W.S., 1986. Iron-silica crystallite nucleation by bacteria in a geothermal sediment. Nature 320, 609–611.

Ferris, F.G., Fratton, C.M., Gerits, J.P., Schultze-Lam, S., Sherwood Lollar, B., 1995. Microbial precipitation of a strontium calcite phase at a groundwater discharge zone near Rock Creek, British Columbia, Canada. Geomicrobiol J. 13, 57–67.

Flynn, S.L., Szymanowski, J.E.S., Fein, J.B., 2014. Modeling bacterial metal toxicity using a surface complexation approach. Chem. Geol. 374, 110–116.

Fowle, D.A., Fein, J.B., 1999. Competitive adsorption of metal cations onto two gram positive bacteria: testing the chemical equilibrium model. Geochim. Cosmochim. Acta 63, 3059–3067.

Haas, J.R., Dichristina, T.J., Wade, R., 2001. Thermodynamics of U(VI) sorption onto *Shewanella putrefaciens*. Chem. Geol. 49, 609–611.

Jones, B., Konhauser, K., Renaut, R.W., Wheeler, R., 2004. Microbial silicification in Iodine Pool, Waimangu geothermal area, North Island, New Zealand: implications for recognition and identification of ancient silicified microbes. Geol. Soc. Lond. 161, 983–993.

Kolter, R., Greenberg, P.E., 2006. Microbial sciences: the superficial life of microbes. Nature 441, 300–302.

Konhauser, K.O., 2007. Introduction to Geomicrobiology. Blackwell Publishing, Oxford, UK.

Konhauser, K.O., Urrutia, M.M., 1999. Bacterial clay authigenesis: a common bacterial process. Chem. Geol. 161, 399–413.

Konhauser, K.O., Fisher, Q.J., Fyfe, W.S., Longstaffe, F.J., Powell, M.A., 1998. Authigenic mineralization and detrital clay binding by freshwater biofilms: the Brahmani River, India. Geomicrobiol J. 15, 209–222.

Kuyucak, N., Volesky, B., 1989. Accumulation of cobalt by marine alga. Biotechnol. Eng. 33, 809–814.

Lalonde, S.V., Amskold, L., Warren, L.A., Konhauser, K.O., 2007. Surface chemical reactivity and metal adsorptive properties of natural cyanobacterial mats from an alkaline hydrothermal spring, Yellowstone National Park. Chem. Geol. 243, 36–52.

Matheickal, J.T., Yu, Q., Woodburn, G.M., 1999. Biosorption of cadmium (II) from aqueous solution by pre-treated biomass of marine alga *Durvillaea potatorum*. Water Res. 33, 335–342.

Mortimer, R.J.G., Coleman, M.L., Rae, J.E., 1997. Effect of bacteria on the elemental composition of early diagenetic siderite: implications for palaeoenvironmental interpretations. Sedimentology 44, 759–765.

Mullen, M.D., Wolf, D.C., Ferris, F.G., Beveridge, T.J., Flemming, C.A., Bailey, G.W., 1989. Bacterial sorption of heavy metals. Appl. Environ. Microbiol. 55, 3143–3149.

Mullen, M.D., Wolf, D.C., Beveridge, T.J., Bailey, G.W., 1992. Sorption of heavy metals by soil fungi *Aspergillus Niger* and *Mucor Rouxii*. Soil Biol. Biochem. 24, 129–135.

Nealson, K.H., Tebo, B.M., Rosson, R.A., 1988. Occurrence and mechanisms of microbial oxidation of manganese. Adv. Appl. Microbiol. 33, 279–318.

Newman, D.K., Beveridge, T.J., Morel, F.M.M., 1997. Precipitation of arsenic trisulfide by *Desulfotomaculum auripigmentum*. Appl. Environ. Microbiol. 63, 2022–2028.

Ngwenya, B.T., Sutherland, I.W., Kennedy, L., 2003. Comparison of the acid–base behavior and metal adsorption characteristics of gram-negative bacterium with other strains. Appl. Geochem. 18, 527–538.

Okumura, M., Yasushi, M., 1986. Coprecipitation of alkali metal ions with calcium carbonate. Geochim. Cosmochim. Acta 50, 49–58.

Rainey, R.K., Jones, B., 2009. Abiotic versus biotic controls on the development of the Fairmont Hot Spring carbonate deposite, British Columbia, Canada. Sedimentology 56, 1832–1857.

Sadiq, M., 1992. Basic concepts in Marine Chemistry. Toxic Metal Chemistry in Marine Environments. Marcel Dekker Inc., New York, pp. 5–29.

Schofield, E.J., Veeramani, H., Sharp, J.O., Suvorova, E., Latmani, R.B., Mehta, A., Stahlman, J., Webb, S.M., Clark, D.L., Conradson, S.D., Ilton, E.S., Bargar, J.R., 2008. Structure of biogenic uraninite produced by *Shewanella onedensis* strain MR-1. Environ. Sci. Technol. 42, 7898–7904.

Schultze-Lam, S., Beveridge, T.J., 1994. Nucleation of celestite and strontionite on a cyanobacterial S-layer. Appl. Environ. Microbiol. 60, 447–453.

Small, T.D., Warren, L.A., Roden, E.E., Ferris, F.G., 1999. Sorption by bacteria, Fe(III) oxide, and Bacteria-Fe(III) oxide composites. Environ. Sci. Technol. 33, 4465–4470.

Southam, G., Beveridge, T.J., 1994. The in vitro formation of placer gold by bacteria. Geochim. Cosmochim. Acta 58, 4527–4530.

Spath, R., Flemming, H.C., Wuertz, S., 1998. Sorption properties of biofilms. Water Sci. Technol. 37, 207–210.

Teitzel, G.M., Parsek, M.R., 2003. Heavy metal resistance of biofilm and planktonic *Pseudomonas aeruginosa*. Appl. Environ. Microbiol. 69, 2313–2320.

Thompson, J.G., Ferris, F.G., 1990. Cyanobacterial precipitation of gypsum, calcite, and magnesite from natural alkaline lake water. Geology 18, 995–998.

Volesky, B., Holan, Z.R., 1995. Biosorption of heavy metals. Biotechnol. Prog. 11, 235–250.

Warchola, T.J., Flynn, S.L., Robbins, L.J., Liu, Y., Meyers, R., Gauger, T., Kovalchuk, O., Alam, M.S., Wei, S., Lalonde, S.V., Kappler, A., Alessi, D.S., Konhauser, K.O., 2017. Field- and lab-based potentiometric titrations of microbial mats from the Fairmont Hot Springs, Canada. Geomicrobiol J. (in review).

Warren, L.A., Maurice, P.A., Parmar, N., Ferris, F.G., 2001. Microbially mediated calcium carbonate precipitation: implications for interpreting calcite precipitation and for solid phase capture of inorganic contaminants. Geomicrobiol J. 18, 93–115.

Xue, H.B., Stumm, W., Sigg, L., 1988. The binding of metals to algal surfaces. Water Res. 22, 917–926.